Critical factors determining the variation in SOA yields from terpene ozonolysis: A combined experimental and computational study

Neil M. Donahue,*[a] Kara E. Huff Hartz,[a] Bao Chuong,[a] Albert A. Presto,[b] Charles O. Stanier,[c] Thomas Rosenhørn,[d] Allen L. Robinson[e] and Spyros N. Pandis[bf]

[a] *Departments of Chemistry and Chemical Engineering, Carnegie Mellon University, Pittsburgh PA 15213, USA. E-mail: nmd@andrew.cmu.edu*
[b] *Department of Chemical Engineering, Carnegie Mellon University, Pittsburgh PA 15213, USA*
[c] *Department of Chemical Engineering, University of Iowa, Iowa City IA 52242, USA*
[d] *Department of Chemistry, University of Copenhagen, DK-2100, Copenhagen, Denmark*
[e] *Department of Mechanical Engineering, Carnegie Mellon University, Pittsburgh PA 15213, USA*
[f] *Department of Chemical Engineering, University of Patras, Patras GR-26500, Greece*

Received 16th November 2004, Accepted 14th February 2005
First published as an Advance Article on the web 17th May 2005

A substantial fraction of the total ultrafine particulate mass is comprised of organic compounds. Of this fraction, a significant subfraction is secondary organic aerosol (SOA), meaning that the compounds are a by-product of chemistry in the atmosphere. However, our understanding of the kinetics and mechanisms leading to and following SOA formation is in its infancy. We lack a clear description of critical phenomena; we often don't know the key, rate limiting steps in SOA formation mechanisms. We know almost nothing about aerosol yields past the first generation of oxidation products. Most importantly, we know very little about the derivatives in these mechanisms; we do not understand how changing conditions, be they precursor levels, oxidant concentrations, co-reagent concentrations (*i.e.*, the VOC/NO_x ratio) or temperature will influence the yields of SOA. In this paper we explore the connections between fundamental details of physical chemistry and the multitude of steps associated with SOA formation, including the initial gas-phase reaction mechanisms leading to condensible products, the phase partitioning itself, and the continued oxidation of the condensed-phase organic products. We show that SOA yields in the α-pinene + ozone are highly sensitive to NO_x, and that SOA yields from β-caryophylene + ozone appear to increase with continued ozone exposure, even as aerosol hygroscopicity increases as well. We suggest that SOA yields are likely to increase substantially through several generations of oxidative processing of the semi-volatile products.

DOI: 10.1039/b417369d

1. Introduction

The objective of this paper is to pose, and *begin* to answer, a simple question. *If we wish to know the yield of secondary organic aerosol from terpenes, and how it varies with specific compounds and changing ambient conditions, to what extent do we need to understand the elementary reactions and particle physics that comprise this enormously complicated process?* We shall argue that substantially detailed understanding is necessary, but that certain key points require particular attention. Our vehicle will be a journey through current research into cycloalkene ozonolysis and organic particle heterogeneous oxidation, beginning with the fundamental reaction dynamics of substituted cyclohexenes and ending with a discussion of aerosol yields through successive generations of organic particle oxidation.

Terpenes are extremely important biogenic hydrocarbons. They are made up of multiple isoprene units, and while their combined flux into the atmosphere appears to be much smaller than that of isoprene, two characteristics appear to give them disproportionate influence over tropospheric chemistry. First, they can be highly reactive. Like isoprene, they react with OH radicals on nearly every collision.[1] However, unlike isoprene many have very high ozone rate constants as well; some sesquiterpene–ozone rate constants are as large as the *A*-factor for a typical ring-forming ozonolysis reaction.[2] This high reactivity with ozone raises the potential for a strong local nonphotolytic source of OH radicals,[3] which has been invoked as a possible cause for nocturnal OH observations.[4] Second, the oxidation products of the terpenes can have very low vapor pressures, condensing on existing aerosols to form Secondary Organic Aerosol (SOA) or, possibly, nucleating to form fresh particles.[5] Many of these oxidation products are semi volatile, meaning that they exist substantially in both gas and condensed phases in the atmosphere. Experimental evidence shows that ozonolysis of terpenes is an especially efficient source of SOA.[6] It is also clear that some of the condensed products combine to form higher molecular weight, lower vapor pressure material in the condensed phase.[7,8] Finally, almost all of the oxidation products remain substantially reduced; consequently they are subject to continued oxidation, in either the gas or the condensed phase. This oxidation may further reduce the vapor pressure of the product mix by adding polar functionality to the products, or it may increase the vapor pressure by cleaving carbon–carbon bonds and producing relatively low molecular weight compounds that return to the gas phase.

There is always a tension between the desire for a detailed understanding of oxidation mechanisms rooted in elementary kinetics and a need to constrain and parameterize reaction products or their physical and chemical properties before such a detailed understanding is established. Furthermore, it is unimaginable that we will ever be able to assemble a detailed oxidation mechanism capable of accurately predicting yields of successive generations of products under the complete range of atmospheric conditions solely *via* elementary reaction kinetics. Propagation of error would rapidly overwhelm any such attempt. However, larger-scale process studies in environmental chambers are famously vulnerable to fatal interferences from secondary chemistry and wall reactions. Clearly, efforts to understand the oxidation of complex species such as the terpenes must combine both elementary and chamber studies, and often computational studies as well.

Ozonlysis presents especially vexing complexity for at least two basic reasons. First, important parts of the mechanism are non thermal, involving substantial chemical activation and collisional stabilization, in some cases after several generations of isomerization and decomposition. As carbon number increases, both stabilization and aerosol yields will tend to increase; however, the degree to which specific yields depend on mechanistic changes caused by differing degrees of stabilization or simply lower vapor pressures of otherwise analogous products is unknown. Also the different role of endocyclic and exocyclic double bonds is only partly understood. Second, the relatively rapid reaction of ozone with NO has limited the ability of chamber studies to isolate ozonolysis reactions from the mixed photochemistry involving ozone, OH radicals, and photolysis, except under NO_x-free conditions. As ozonolysis of terpenes may be a major source or organic particulate matter is is essential that we develop an accurate understanding of SOA yields from terpene ozonolysis. The dependence on NO_x levels is especially interesting, both because of the lack of experimental understanding and because it has policy implications; if aerosol yields vary significantly with the VOC/NO_x ratio, and we shall show that they do, NO_x controls will have a potentially significant effect on SOA production.

This discussion paper is organized as a series of vignettes, each illustrated with current research from our group. Each will deal with ozone–alkene reactions, and each will be guided by particle

formation as the theme. We shall start with the potential energy surface, wondering what controls the relative reactivity of different alkenes with ozone, and work our way, ultimately, to the oxidation of successive generations of condensed-phase products in the atmosphere. At each stage we shall focus on some critical questions and on factors coupling that stage to successive stages.

2. The potential energy surface

Our first consideration is the potential energy surface for ozonolysis. The objective is to identify key transition states or intermediates that are either rate determining or product determining. Having done so, we wish to understand how these change from one reaction to another.

The overall rate-determining step appears to be the initial transition state: the 1,3-dipolar cycloaddition of ozone to the double bond to form a primary ozonide (1,2,3-trioxolane, or POZ), as shown in Fig. 1. There are several interesting aspects to this transition state. First, the electronic energy of essentially all of the ozone–alkene barriers is *lower* than the reactant energy, but the significant zero-point energy associated with forming a cyclic transition state results in a zero-point energy corrected barrier slightly above the reactant energy.[3] Second, the observed temperature dependences of ozone–alkene reactions show a systematic variation with the degree of substitution around the double bond, with increasing numbers of electron donating substituents lowering the activation energies.[2,9]

An especially interesting sequence includes 2-methylpropene, 2-methyl-2-butene, α- and β-pinene, and β-caryophylene. Both α-pinene and β-caryophylene are considered in detail throughout this paper. The published rate constant for β-caryophylene ozonolysis is 1.2×10^{-14} cm^3 s^{-1}.[2] This is much higher than the obvious model systems. The endocyclic double bond in β-caryophylene is functionally similar to that of α-pinene, with a *cis*-conformation enforced by the ring and a single methyl substituent on one end of the double bond. The α-pinene rate constant is 8.7×10^{-17} cm^3 s^{-1} with an Arrhenius expression of $(1.0 \times 10^{-15})\exp(-732\ \mathrm{K}/T)$ cm^3 s^{-1}.[2] The 2-methyl-2-butene rate constant, also trisubstituted, is 4.0×10^{-16} cm^3 s^{-1} with an Arrhenius expression of $(6.5 \times 10^{-15})\exp(-829\ \mathrm{K}/T)$ cm^3 s^{-1}.[2] The exocyclic double bond is terminal, as with β-pinene. The β-pinene rate constant is only 1.25×10^{-17} cm^3 s^{-1}.[2] The 2-methylpropene rate constant, also terminal, is 1.2×10^{-17} cm^3 s^{-1} with an Arrhenius expression of $(2.7 \times 10^{-15})\exp(-1632\ \mathrm{K}/T)$ cm^3 s^{-1}.[2]

The activation energies show the expected variation with substitution, with the tri-substituted double bonds showing much lower activation energies than the terminal double bonds. Major details remain to be answered, however; the *A*-factor for α-pinene is much lower than the *A*-factor

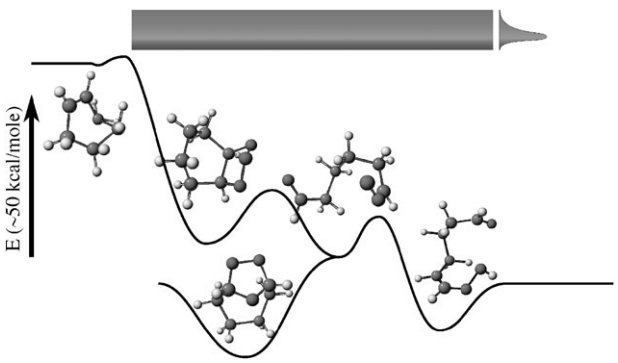

Fig. 1 A typical potential energy surface for ozonolysis of an endocyclic alkene: in this case cyclohexene for simplicity. Nascent reaction products are formed with a Boltzmann distribution of energy defined by the initial transition state (indicated by the colored band). Because endocyclic double bonds lead to a tethered product, this initial energy remains internal to the reaction products, leading to chemically activated behavior. The first linear product contains carbonyl-oxide and carbonyl moities and has at least two possible degradation pathways: formation of a secondary ozonide (SOZ) or formation of a vinyl hydroperoxide (VHP). The VHP/SOZ branching ratio is very energy dependent and thus changes with collisional stabilization.

for 2-methyl-2-butene, perhaps because the attacking ozone is limited to only one of the four potential conformations leading to the POZ. Most significantly, the rate constant for β-caryophylene (and other sesquiterpenes) appears to be anomalously high.

It is probable that the endocyclic double bond in β-caryophylene dominates the observed rate constant, but the physics that drives the progression from 2-methyl-2-butene and α-pinene to β-caryophylene is mysterious. The β-caryophylene rate constant is roughly equal to the *A*-factors for the analogous reactions (and consistent with cycloaddition *A*-factors obtained from transition state theory). Thus this cycloaddition must be essentially barrierless, if indeed it is concerted.

It is tempting to extend the discussion of evolving ozone–alkene rate constants to the high ozone uptake coefficient observed on pure, unsaturated surfaces. The uptake coefficient of ozone on a pure oleic acid surface or aerosol is roughly 10^{-3},[10–12] while the 'uptake coefficient' for β-caryophylene is 10^{-4}, relative to the hard-spheres collision frequency. It may be that large organics, and certainly condensed-phase organics, are able to effectively solvate the ozone, increasing the observed rate constant.

This system is ideal for consideration within the limits of classical transition state theory (TST) as the cyclic transition state makes all of the important modes harmonic (there are no challenging hindered rotors or shallow bend angles). Consequently, if the barrier height and frequencies are known, TST should accurately predict the observed ozonolysis rate constants. This is interesting for several reasons: First, we have recently made substantial progress in understanding barrier height and TST frequency evolution in homologous radical-molecule reactions, focusing on excited states of reactants and products corresponding to a single electron transfer between reagents.[13–15] Second, successful modeling of known ozone–alkene kinetics could illuminate the anomalous behavior of the sesquiterpenes. Third, the cycloreversion transition state out of the POZ is isoelectronic with the cycloaddition and controls the *product* distribution of the reactants. Direct measurements of (thermal) POZ decomposition are very difficult, so there are essentially no data to constrain this critical barrier.

3. Reaction dynamics

The ozonolysis reaction is typically 80 kcal mol^{-1} or more exothermic, and the cycloreversion barrier to formation of a carbonyl oxide and an aldehyde or ketone, though perhaps 15 kcal mol^{-1}, lies some 65 kcal mol^{-1} below the reactant energy. POZ decomposition is thus extremely rapid, and even the resulting fragments, including the 'elusive' carbonyl oxide (Criegee intermediate, or CI), are typically highly vibrationally excited. Endocyclic alkenes add the twist that the cycloreversion fragments are tethered by the carbon ring. This generates two competing effects, illustrated in Fig. 1: first, the chemical activation energy remains localized in the single product; second, a unimolecular pathway to a secondary ozonide (SOZ) exists because the carbonyl and carbonyl oxide moities remain on the same molecule. The importance of this SOZ pathway is under debate,[3,16–18] but we have recently shown that any role of this SOZ pathway will depend critically on the degree of collisional stabilization for the carbonyl oxide.

We have recently modeled the collisional stabilization of a series of substituted cyclohexenes, which serve as a model system for the terpenes. The *A*-factors and energies for the critical transition states shown in Fig. 1 are very different. Because formation of the SOZ involves a bicyclic transition state, but other unimolecular pathways (formation of a vinyl hydroperoxide and thus OH radical or formation of a dioxirane) involve three- and four-member ring transition states, the *A*-factor for SOZ formation is many orders of magnitude lower than the competing transition states. However, SOZ formation is almost barrierless, according to density functional calculations.[3] The consequence is that SOZ formation will dominate at low energy, once the reaction products are collisionally stabilized, but that the other pathways will dominate at high energy. Stabilization scales with pressure and carbon number, and master equation calculations suggest that full stabilization occurs between a carbon number of 10 and 15 for the pathway leading to OH formation (the *syn*-carbonyl oxide) but possibly at a higher carbon number for the dioxirane pathway leading to the 'hot acid' (the *anti*-carbonyl oxide).

Earlier work on linear alkenes shows collisional stabilization at a lower carbon number, apparently between 6 and 10. The difference is that the linear alkenes break into two fragments after the cycloreversion, with each fragment carrying a portion of the excess energy. Even though

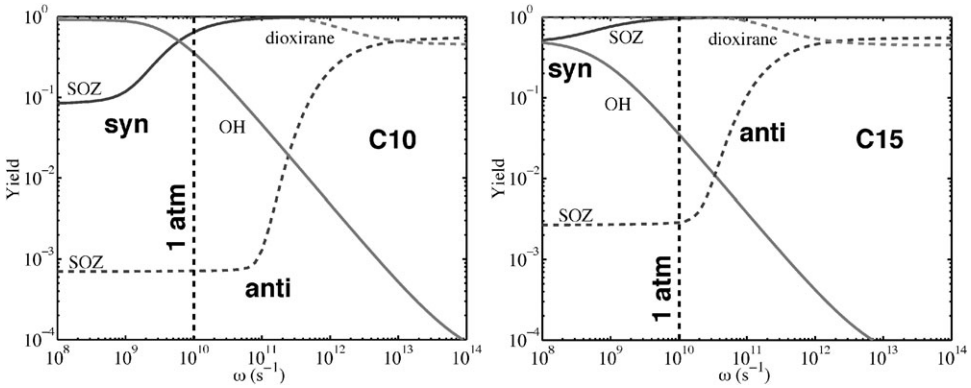

Fig. 2 Collisional stablization and branched reactions in mono- and sesquiterpene model systems. Results are master equation simulations constrained by density functional calculations. Stabilization is shown as a function of collision frequency, with one atmosphere being near 10^{10} Hz. Results are shown for two conformers of the carbonyl oxide (Criegee intermediate): *syn*, which can form a vinyl hydroperoxide and subsequently OH radical, and *anti*, which can form a dioxirane and subsequently an organic acid. Both conformers can also re-cycle to form a secondary ozonide (SOZ) because of the distal carbonyl oxide functionality. Stabilization appears to become important for a carbon number between 10 and 15.

these fragments have a lower carbon number, their lower energy outweighs this, leading to more rapid stabilization.[19,20]

The important conclusions from this work are that we expect a large, qualitative difference in chemical mechanisms from *endo*- and *exo*-cyclic compounds, and that we also expect a sharp change in the chemistry of endocyclic compounds at some critical carbonnumber, when collisional stabilization begins to play a role in these systems. For the endocyclic compounds, our work suggests that this critical carbon number lies between C10 and C15, meaning that the endocyclic monoterpenes are likely to be collisionally activated while the sesquiterpenes will be collisionally stabilized. Other work from our lab shows that linear (and endocyclic) alkenes are stabilized between C6 (*i.e.* tetramethylethylene) and C10 (*i.e. trans*-5-decene).[20] Consequently, we expect that linear or exocyclic systems with SOA formation potential will tend to be collisionally stabilized at 1atm pressure.

4. Reaction mechanisms

Relatively little is known about the detailed chemistry following the initial reaction with ozone. Clearly, whatever organic fragments are produced, they will eventually be collisionally stabilized and may participate in thermal chemical reactions. Potential reactions of the SCI with various compounds, especially water, have received considerable attention recently,[21,22] and certainly some attempts have been made to elucidate basic reaction mechanisms that are at least consistent with end-product observations.[23] The essential point is that ozonolysis may well produce organic fragments that participate in oxidation cycles resembling standard organic oxidation mechanisms.[1] We therefore expect end products to depend on HO_2 : VOC : NO_x ratios, especially if peroxy radicals are found in the mechanisms, and we can generally expect the distribution and volatility of end products to vary with ambient conditions. Based on our modeling of the ozonolysis reaction dynamics, there is a strong possibility that the mechanisms for mono and sesqui terpenes are qualitatively different, with much more fragmentation and subsequent radical chemistry following monoterpene ozonolysis.

Experimental constraints on reaction mechanisms can emerge from three major threads: successive studies of the elementary kinetics of each coupling reaction; experiments that treat a set of reactions connecting a relatively stable precursor to a relatively stable product; and experiments (typically in smog chambers) reproducing the complete set of coupled reactions constituting the complete oxidation sequence. Not only is it impossible to imagine a complete set

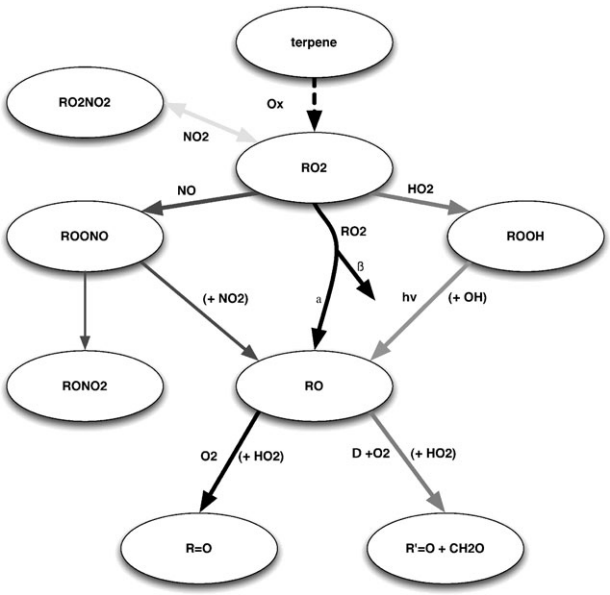

Fig. 3 A schematic illustrating possible NO_x-dependent chemistry following oxidation of terpenes, including ozonolysis. The assumption is that after some unknown series of reactions, an organic radical fragment will eventually combine with molecular oxygen to form a peroxy radical, which will then follow a pattern common to other peroxy radicals. The details of this chemistry are as yet unknown. However, we expect the distribution of products to depend on the VOC/NO_x ratio, primarily because this will alter the fate of the peroxy radicals. This will then influence the distribution of semi-volatile products, and thus aerosol yields.

of accurate kinetics experiments for the full oxidation of numerous terpenes under consideration here, any reasonable propagation of error starting with a terpene precursor and a mix of oxidants would lead quickly to 100% uncertainty in the yields of most products after only a few generations of oxidation. Consequently, most mechanisms are based on smog chamber experiments.[17,24] Unfortunately, these experiments suffer from a similar uncertainty associated with error propagation – measurements in chamber experiments are typically inverted through some form of least-squares fitting to a presumed basic mechanism to yield kinetic parameters. However, it is difficult to find a unique solution, and often secondary reactions not important in the ambient atmosphere can interfere, especially when concentrations are elevated to improve signal to noise. We have favored studies in flow tubes, with timescales ranging from 100 msec to 1 minute and well-controlled oxidant concentrations.[25] This allows a mechanism to be broken into individual steps connecting a precursor to the first generation of stable products – for example in the OH oxidation of isoprene.[26] These experiments can provide a critical link between elementary kinetics measurements and chamber experiments; they are typically designed to focus on a critical branch point in the oxidation mechanism, such as the reactions of peroxy radicals depicted in Fig. 3.

4.1. Mechanisms from an engineering perspective

The detailed oxidation mechanisms of most SOA precursors are not known. Furthermore, in some sense the specific identity of the reaction products is less important than their vapor pressure, at least for the narrowly defined problem of SOA production. Consequently, it is useful to think of the overall mechanism for the reaction of a precursor VOC_i with an oxidant Ox as a reduced expression of the form.[27–29]

$$\mathrm{VOC}_i + \mathrm{Ox} \xrightarrow{K_{i,\mathrm{Ox}}} \sum_j \alpha_{i,j} p_j \qquad (1)$$

where $k_{i,\mathrm{Ox}}$ is the rate-limiting rate constant, $\alpha_{i,j}$ is a molar yield, and p_j is a product (or a group of products with similar vapor pressures). The question at the heart of this paper is: How much fundamental detail is required to produce accurate mechanisms of this sort (extending to multiple generations), and how can constraints from multiple layers of complexity be integrated to give an accurate representation of SOA yields in the atmosphere?

5. Particle formation

We need to constrain aerosol formation. This adds a dimension to the problem: phase equilibria. We are not addressing particle number. There are indications that organics rarely if ever actually nucleate to form new particles in the atmosphere but rather condense on to existing inorganic or mixed particles.[29,30] Nonetheless, we need to know the saturation vapor pressure of a complex mix of compounds over an equally complex condensed phase.

Qualitatively, some reaction products will have high vapor pressures. These, such as CO, CO_2, CH_2O, and many larger species as well, will be completely volatile. Some other products will have extremely low vapor pressures. These, like sulfate, will have negligible mass fractions in the gas phase and will thus be completely non-volatile. However, with SOA a substantial fraction of the products will be of intermediate volatility, existing at or near their saturation vapor pressures and thus partitioning substantially into both the gas and condensed phases. These compounds are semi volatile. This general scheme is summarized in Fig. 9 later in this paper.

The semi-volatile compounds pose a substantial challenge, which is exacerbated by recent findings of substantial oligomerization in the condensed phase.[7,8] The universal approach has been to assume pseudo-ideal solution theory.[27] However, even with this assumption there are several hurdles to clear before accurately predicting partitioning. In theory, if one could completely describe the oxidation mechanism, one could simply assemble an ideal solution comprised of the reaction products under a given set of conditions and model the partitioning. Even in relatively well-studied systems like α-pinene, we don't know the mechanisms well enough to do this; as we shall discuss in the next section, an especially vexing gap is our crude understanding of the coupling of the ozonolysis mechanism with NO_x. Even if we did know the mechanisms well, we don't know the phase behavior of most products; many have never been synthesized, and the very low vapor pressures are quite difficult to measure. The most important parameter in each case is the heat of vaporization, and this should determine the temperature dependence of the phase partitioning. This temperature dependence is a leading source of uncertainty in regional SOA models.[31] Coupled, perhaps, to oligomerization is the general observation that SOA appears to be both less volatile and yet less sensitive to temperature than known vapor pressures of pure major constituents would suggest.[29]

An alternate approach is to use ideal partitioning of an arbitrary number of products as a template for fitting measured yields. Conceptually, this aggregates products into groups with similar vapor pressures. This greatly reduces the complexity of the mechanism needed to model SOA formation, but of course it also obliterates any specific information about product distributions. In practice, experiments most often constrain SOA yields over a range of initial precursor concentrations. Semi-volatile products will partition progressively toward the condensed phase with larger initial loadings. In a typical experiment (Fig. 4), we measure the SOA yield by measuring the evolving spectrum of particle mobility diameters using a Scanning Mobility Particle Sizer (SMPS): particle mass is inferred assuming spherical particles with a density of 1 g cm^{-3}.

In most cases yield data at a single temperature covering a wide range of precursor concentrations can be fit with a two-component model containing a relatively volatile and a relatively non-volatile component.[27,28] However, these single-temperature experiments do not constrain the heat of vaporization of those components. For this constraint we employ a temperature-controlled smog chamber. We hold the oxidation temperature constant at 25 °C, then vary the temperature from 15–40 °C after oxidation and particle formation is complete.[29]

The end result of this approach for α-pinene is shown in Fig. 5. The SOA volume increases as temperature decreases, but quite modestly, by about 2% K^{-1}. Detailed modeling synthesizing these temperature-dependent data with extensive data covering the partitioning at room temperature over a wide range of reacted α-pinene reveals two things.[29] First, three major products and one minor component are required to fit the combined data, as the standard two-component model[27,28] cannot

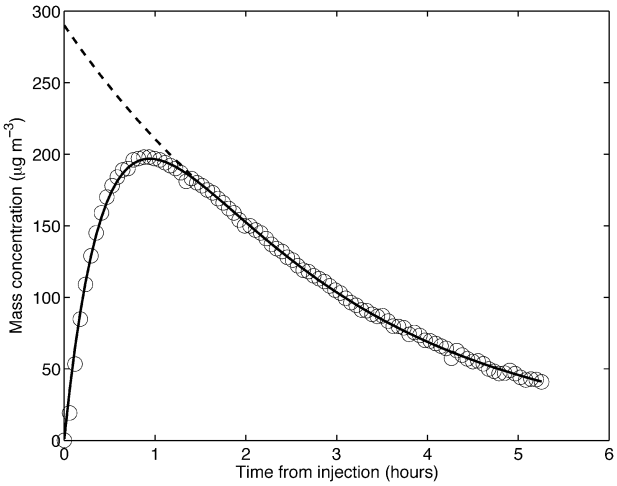

Fig. 4 A typical SOA yield experiment for α-pinene + ozone in the presence of an OH scavenger (2-butanol). Particle mass is determined with an SMPS. The particle formation timescale is determined by a combination of oxidation and nucleation kinetics, while the decay is due to wall loss. Semi-volatile material on the wall remains active in phase partitioning. The measured yield is thus found by extrapolating the decaying portion of the mass curve back to $t = 0$, when the reaction was initiated.

simultaneously capture the concentration and temperature dependence of the partitioning. These components arise from a fitting procedure initialized with nine components, most of which emerge with near zero yields from the optimization. Second, the effective enthalpy of vaporization required to reproduce the gentle temperature dependence observed is 30 kJ mol^{-1}. This is much less than the

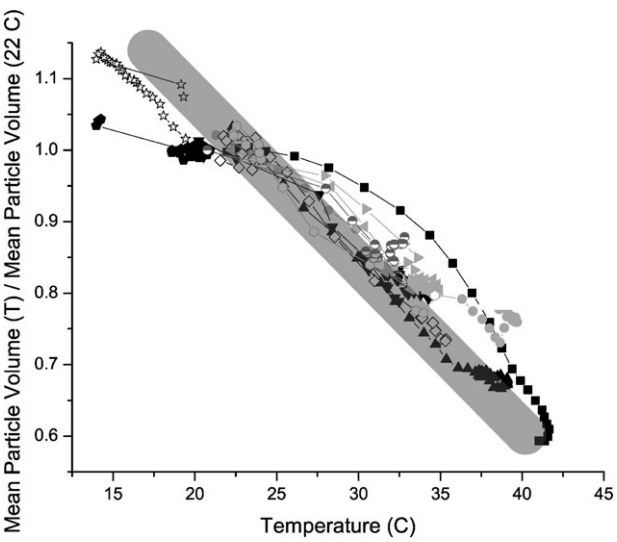

Fig. 5 Summary of α-pinene + ozone SOA yield experiments in the absence of NO_x. After reaction at 25 °C, the chamber temperature was varied from 15 to 40 °C and the change in aerosol mass measured. No systematic difference between upward and downward temperature ramps was observed. Data are normalized to the SOA yield at 23 °C to show the fractional change in SOA mass with changing temperature. The total oxidized α-pinene varies from 15 to 150 ppbv, but despite significantly different absolute yields with total reacted α-pinene, the change with temperature shows no systematic dependence on the amount of condensible products. Within error, the data are consistent with a temperature dependence of 2%/K, as shown with the thick diagonal stipe. This corresponds to a mean 'vaporization temperature' of 1800 K, or 15 kJ mol^{-1}.

100–120 kJ mol^{-1} typical of individual components generally thought to comprise most of the semi-volatile products from α-pinene. Either this reflects the net effect of a more diverse actual product distribution, or there is another physical or chemical phenomenon controlling aerosol partitioning with this net temperature dependence. We are exploring whether reversible dimerization with a free energy difference of approximately 30 kJ mol^{-1} could explain these observations.

6. NO_x and aerosols

We know that odd nitrogen can significantly influence hydrocarbon oxidation mechanisms.[1] We know relatively little about the NO_x dependence of the chemistry following ozonolysis mostly because it is difficult to design experiments that isolate it. Specifically, ozone and NO_x react, and ozone alkene chemistry tends to produce OH radicals. Thus, while many studies have considered the total oxidation of precursors such as β-pinene,[32] these studies generally conflate ozone and OH oxidation mechanisms, making mechanistic insight difficult to obtain. Consequently, published oxidation mechanisms for terpenes tend to have detailed descriptions of the mechanisms following OH attack, but quite crude descriptions of any chemistry following ozone attack.[23]

It is often assumed that the organic fragments will follow an oxidation sequence similar to the standard progression for organic radicals, involving formation of peroxy radicals and their subsequent interactions with other peroxy radicals (including HO_2) as well as NO_x. This basic scheme is illustrated in Fig. 3. Even before we have completely elucidated the mechanisms at this critical branch point, we can conclude that we might expect particle yields following ozonolysis of terpenes to depend on the peroxy radical branching. The most common surrogate for this is the VOC/NO_x ratio.

In order to constrain the VOC/NO_x dependence of aerosol production, we have followed the ozone–α-pinene reaction in a 10 m^3 teflon reactor containing ample 2-butanol to scavenge any OH radicals. Typical results are shown in Fig. 6 for two different initial α-pinene concentrations. The increase in yields with increasing α-pinene oxidized is entirely consistent with previous observations[28,29] – this is because most of the products are semi volatile, and increased total concentrations force material into the condensed phase. However, SOA yields also drop dramatically once VOC/NO_x drops below 10 ppbC/ppbNO_x (values from 2 to 10 are common in urban and regional

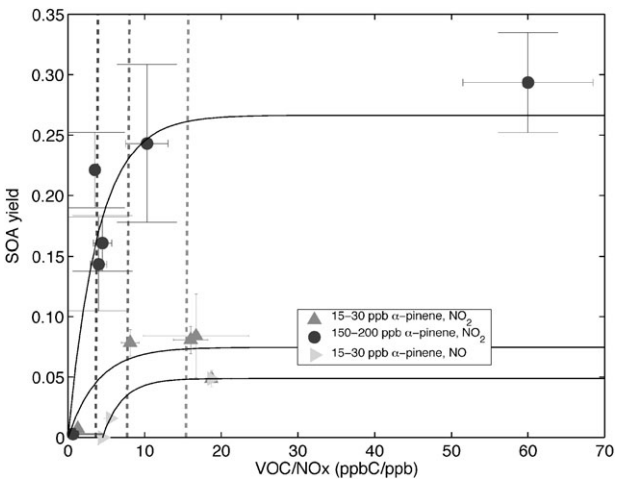

Fig. 6 Aerosol yields as a function of VOC/NO_x from α-pinene + ozone, with 2-butanol added as a radical scavenger. Yields are constant at low NO_x but decrease sharply as NO_x increases (lowering VOC/NO_x to less than 10 ppbC/ppbNO_x). VOC/NO_x values of 4 : 1, 8 : 1, and 16 : 1 are shown as vertical dashed lines; these values are typical for VOC-limited, transitional, and NO_x-limited conditions for urban ozone production. Both NO_2 and NO reduce SOA yields, but the effect is most dramatic for NO, culminating in a complete disappearance of SOA production for 10 ppbv of initial α-pinene at a VOC/NO_x of 5 : 1. This suggests that yields obtained from NO_x-free experiments may be a factor of 5 or more higher than those under typical ambient conditions.

environments). This strongly suggests that mechanisms neglecting this chemistry overpredict SOA yields from α-pinene ozonolysis. The extent of this overprediction is unclear, as terpene sources are often not co-located with NO_x sources; consequently, the necessary modeling studies are ongoing. However, where terpene oxidation occurs in the presence of an urban plume the reduction could be a factor of five or more.

For most of these experiments NO_x was primarily NO_2. While one might expect the chemistry to change dramatically with NO/NO_2 closer to ambient levels, experiments with NO show a similar but more dramatic effect, shown in the lowest curve of Fig. 6. These experiments must be performed with UV lights on in our chamber to convert NO_2 produced in the O_3 + NO reaction back to NO. This shows a complete elimination of aerosol formation at a VOC/NO_x of 5 for 20 ppb initial α-pinene. This suggests that none of the major products had a saturation vapor pressure lower than 20 ppb. GC/MS data from these experiments also shows higher yields of higher volatility products as VOC/NO_x decreases (*i.e.*, as NO_x increases).[33]

Another intriguing finding is that observed SOA yields drop by a roughly constant 0.03 in the presence of UV, consistent with the photolysis of an intermediate in the gas-phase replacing a relatively non-volatile product with a much more volatile product.[34] This effect can be seen in the downward offset of the lowermost curve in Fig. 6 from the curve immediately above it, which was obtained at a similar VOC level but in the dark.

There are two major possibilities for the observed changes in aerosol yields. First, the distribution of products may change, as we observe with the GC/MS. Second, entirely new products may be produced, such as organic nitrates. If these are more volatile than the products they replace, once again the aerosol yields will decrease. In fact, we do observe substantial nitrate formation in FTIR spectra of teflon filters drawn during these experiments, and the nitrate features decline more rapidly than carbonyl features as the filters are heated.[33]

From this point we can move in two directions. First, detailed experiments are needed to isolate the key branchpoints in the mechanism responsible for this change in particle yields. Second, however, we need parameterized mechanisms such as those depicted in eqn. (1) for use in air quality models and to condense the incredible detail of the full mechanism. Both steps are crucial – we can't be confident in the condensed mechanism without detailed understanding, but we can't proceed with the full complexity of this problem with a master mechanism either. Clearly SOA yields are very sensitive to ambient conditions, even for ozonolysis, where most existing models assume that yields are constant.

7. Aerosol heterogeneous oxidation

Finally, when we discuss aerosol yields, it is clear that we can not confine ourselves to a single generation of gas-phase oxidation. This brings a final layer of complexity to the problem, as we must consider not just a single, multi-step oxidation mechanism, but the full succession of mechanisms for the partially oxidized products. Furthermore, the oxidation will occur in both gas and condensed phases. Still, the simple question being asked here is the ultimate mass yield of condensed-phase material somewhere downwind of a source; the specific composition of the products is not *directly* relevant.

7.1. Aging of ambient aerosols

The typical lifetime of atmospheric aerosols is of order one week: for example if we assume a mean deposition velocity for particles (including average wet deposition) of 0.3 cm s^{-1} and a mean mixed layer height of 1 km, the deposition timescale is

$$\tau_{dep} = \frac{H}{v_{dep}} = 3.8 \text{ d}$$

During that time, the organic aerosol will be subject to attack by gas-phase oxidants. This we call aging. The dominant oxidant for aerosol aging will be OH radical, for the simple reason that CH_2 groups dominate the chemical composition of organic aerosol,[35] and we expect OH to be the sole effective oxidant of CH_2.

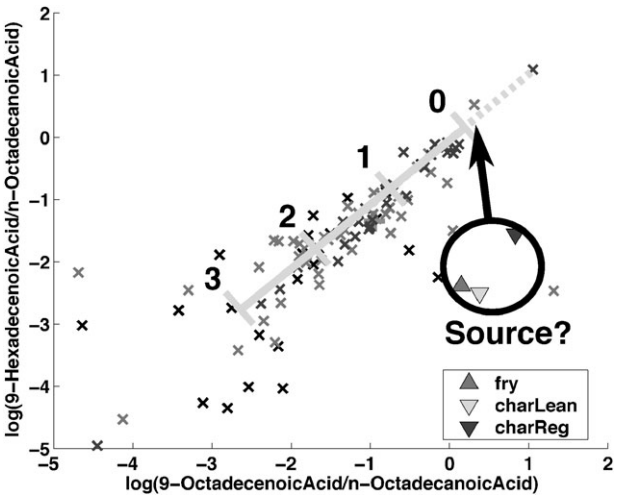

Fig. 7 Alkenoic acids in Pittsburgh: palminoleic (8-hexadecenoic) acid on the *y*-axis, and oleic (9-octadecenoic) acid on the *x*-axis, normalized by steric (*n*-octadecanoic) acid. The natural logs of the concentration ratios are plotted. Meat cooking is a major source. Known cooking sources underestimate palminoleic acid by roughly one order of magnitude; the data suggest a source point as indicated with the black arrow. Subsequent oxidation through approximately exp(−3) is shown as a heavy diagonal line.

It can be argued that ozone might dominate the oxidation of organic aerosol, consuming all unsaturated compounds well before saturated organics are oxidized, but there is considerable empirical evidence that this is not so. Instead, it appears that the timescales associated OH and ozone attack are similar.[36] Several recent experiments focused on ozone uptake to well prepared surfaces[10] and also reduced compound removal[11,12] show very high uptake coefficients, of order 10^{-3}, for ozone to oleic acid, an important component of meat cooking. For typical urban ozone levels, this would lead to an oleic acid lifetime in ambient aerosol of a few minutes,[36] leaving negligible steady-state concentrations. However, ambient observations during the Pittsburgh Air Quality Study clearly show substantial levels of alkenoic acids, as seen in Fig. 7. Rather than presenting a time series, we show a relative kinetics analysis, similar to those employed with gas-phase nonmethane hydrocarbons to determine the photochemical age of an airmass.[37] Specifically, we take filter measurements of two similar alkenoic acids, palmitoleic and oleic acid, and divide each measurement by the corresponding level of an alkanoic acid, steric acid, which is thought to have a similar source. This removes single-source variability from the data, leaving only photochemical processing and mixing of different sources to drive variability. Processing is expected to drive data from a source point down toward the lower left on these log–log plots, with a slope equal to the ratio of the corresponding rate constants (presumably unity in this case). Such a slope is seen here, but with a net decay only e^{-2} to e^{-3}, suggesting an alkenoic acid atmospheric lifetime of somewhat less than 1 d.

The ozone uptake coefficient consistent with this sort of oxidation timescale is of order 10^{-6}, three orders of magnitude lower than what is measured in the laboratory.[36] The clear conclusion here is that some property of real, ambient aerosol greatly reduces the oxidation rate of at least some unsaturated compounds. Whether this is a solvent effect on the cycloaddition barrier, a physical effect (sequestration of the olefin in a secondary phase within the aerosol), or some other phenomenon is not yet known. Neither is the degree of complexity needed to produce this inhibition known, though there are indications that even some two-component mixtures can show this effect.[38] However, it is clear that the effect is intrinsic to the complexity of ambient aerosol.

Calculations suggest that saturated organics in the condensed phase will typically have lifetimes against oxidation by OH of order 1 d as well.[36] It is because the majority of the mass of organics is CH_2 that the overall mass oxidation will thus be dominated by OH.

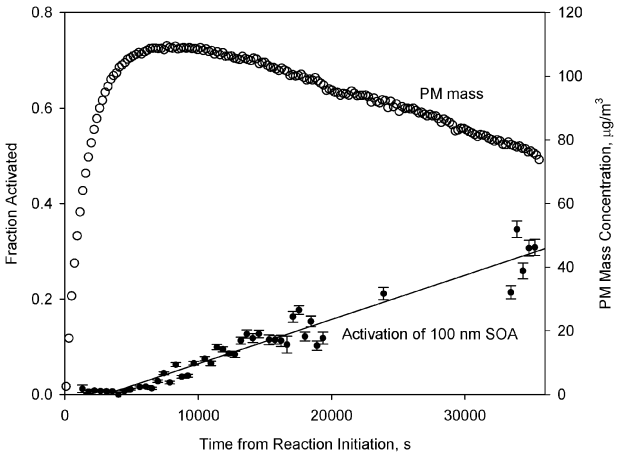

Fig. 8 Cloud condensation efficiency of aerosol particles generated by the ozonolysis of β-caryophylene. Initial conditions are 200 ppbv ozone and 50 ppbv β-caryophylene. 2-Butanol is added as a gas-phase OH radical scavenger.

7.2. Organic aerosol properties: cloud nucleation

We are interested in aerosol production for more reasons that simply aerosol mass. Another bulk property of tremendous importance is the ability of particles to serve as cloud condensation nuclei (CCN). Earlier work at Carnegie Mellon has shown that many organics are excellent CCN.[39–41] Not surprisingly, CCN activity is related to the oxidation state and solubility of organics, with highly water-soluble, polar organics activating efficiently according to Kohler theory.[40] However, the organics are also clearly more complicated than simple inorganic salts; solubility is an issue, and yet some compounds appear to act as good CCN even though their bulk solubilities are low.[40,41]

SOA is often a good CCN, because it is by definition oxidized. However, the oxidation products of larger hydrocarbons, such as β-caryophylene, are still substantially non-polar. They thus show only modest activation.[42] If one follows the activation efficiency of β-caryophylene derived SOA after continued exposure to ozone, however, one sees a monotonic increase in activation. Fig. 8 shows the SOA particulate mass from β-caryophylene following ozone exposure at time zero and also the fraction of 100 nm particles, selected with a differential mobility analyzer, that activate in a cloud condensation nucleus counter held at 1% supersaturation. After an induction period of nearly 5000 s during which none of the 100 nm particles activate (and the PM mass reaches a maximum), the activating fraction proceeds to increase monotonically, and roughly linearly, reaching 45% by the end of the experiment at 36 000 s (10 h). By this same time, the particle mass has dropped by roughly one-third due to wall loss.

Several interesting facts fall out of these data. First, new particles are formed much more slowly than β-caryophylene is oxidized. Given this high rate constant, the lifetime of β-caryophylene in the presence of 200 ppb ozone is approximately 15 s. This presumably yields a linear product, which according to our computational work may well cyclize to form a secondary ozonide.[3] Whatever the product, it will retain a terminal double bond. The ozonolysis rate constant for this compound should be at least 1.2×10^{-17} cm^3 s^{-1}, leading to a (gas-phase) lifetime of 15 000 s. This is considerably longer than the timescale for particle formation, which is in turn much longer than the chemical lifetime of the β-caryophylene precursor. We can thus conclude that the particle formation is rate-limited by nucleation kinetics, though it is quite possible that nucleation is seeded when a small fraction of secondary oxidation generates very low vapor pressure seed particles.

After new particle formation, two other things can be seen in Fig. 8. First, there is a dramatic increase in the CCN activity of the selected 100 nm aerosol. This is presumably chemically driven. Second, the first-order decay timescale of the aerosol is very long, of order 20 h. This is in contrast to the normal wall loss lifetime of aerosol in our 10 m^3 chamber, which is 2–3 h. It is thus possible that there is continued condensation of gas-phase semi-volatile material onto the aerosol

throughout the experiment. This can't be due to the condensation kinetics themselves, so it must be driven by chemistry. It it reasonably consistent with the timescale for secondary ozonolysis in the gas phase, making this a likely candidate. However, it is nearly impossible to determine whether this secondary oxidation actually occurs in the gas or condensed phase: unless the products change, it will make no difference to the SOA yield. It is also possible that the increased CCN activity is driven by a unimolecular process: perhaps isomerization of a relatively volatile secondary ozonide into a less volatile organic acid.

Whatever the cause of these changes, this vignette illustrates that continued chemical processing of initial products, possibly in both gas and condensed phases, can influence the physical properties of organic aerosol. There is also a strong suggestion that this continued processing can significantly increase the overall aerosol yields.

7.3. Generations of oxidation and aerosol yields

If we need to consider successive generations of oxidation for organic aerosols, what will the yields be through those generations? Two forces will fight each other. Obviously, carbon oxidation heads toward a thermodynamic endpoint of CO_2, which is completely volatile. Equally obvious, however, is that the first generation of oxidation experienced by the large precursors (terpenes) under consideration here *decreases* the vapor pressure of most of the products, on a carbon basis: a volatile terpene precursor produces SOA in the first generation with yields ranging from 0.03–1.0. Clearly, in the first generation of products from α-pinene a very substantial portion of the carbon is likely to remain in the gas phase at typical levels of organic aerosol (typically 1–30 μg m^{-3}). However, as the saturation plots such as Fig. 6 reveal, many of these products hover near saturation. There is clearly great potential for further oxidation to push them over the edge into the condensed phase. Is this potential realized in the atmosphere?

We can pose another question: *At what generation will the SOA yield from a given precursor reach a maximum, and what will that yield be?* The factors influencing this partitioning are illustrated in Fig. 9. Ultimately, two major forces compete. Carbon–carbon bond cleavage will produce lighter, more volatile products, while oxygenation will tend to produce polar, less volatile products. In addition, oxygenation will increase the *absolute* aerosol mass, which is the more common operational definition of aerosol yield (we are focusing on carbon mass here). Assuming that yields are determined by equilibrium thermodynamics, it can't matter *where* the oxidation takes place, unless the gas- and condensed-phase mechanisms differ significantly. Finally, aerosol deposition will tend to drive semi-volatile compounds out of the condensed phase as the total mass of material is reduced: that effect is not considered here.

A key parameter in the overall aerosol yield will be the generation number, depicted in Fig. 9, though the change in yield with generation number, $\partial Y/\partial n$ is completely unknown. Even the sign is not known. We are aware of no data that can yet significantly constrain this parameter. However, we can speculate that, if condensed-phase oxidation by OH radicals dominates aerosol aging, increased polarity will substantially outweigh carbon–carbon cleavage, especially when total mass is

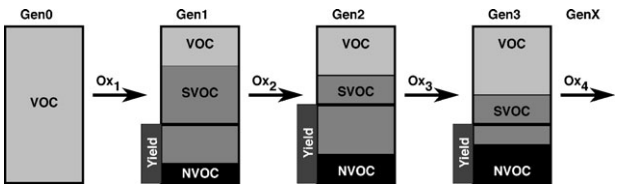

Fig. 9 Aerosol yields through generations of oxidation. The bars represent the carbon mass through successive generations: light gray indicates completely volatile material, dark gray semi-volatile compounds, and black completely non-volatile compounds. A horizontal black line indicates the partitioning between gas and condensed phases in the semi-volatile fraction, and the smaller gray bar shows the total aerosol yield. If oxidation tends to cleave carbon–carbon bonds, it will increase product vapor pressures and thus decrease aerosol yields. If oxidation tends to add polar functionality, it will decrease product vapor pressures and thus increase aerosol yields. In this illustration, successive generations of oxidation increase both the volatile and non-volatile fractions, but also alter the mix of vapor pressures in the semi-volatile fraction, leading to a maximum yield after the second generation of oxidation.

considered, where the carbon fraction of aged aerosol appears to be as low as 0.5. Consequently, it is very possible that the effective yield of aerosol products from many precursors, certainly the monoterpenes, will approach unity within few enough generations to be atmospherically noteworthy. This is entirely consistent with recent observations of isoprene-derived aerosol in remote regions dominated by peroxy radical chemistry.[43] That production is essentially the consequence of successive generations of gas-phase oxidation leading to low vapor pressure tetrols, in spite of relatively volatile first-generation products. It is also quite consistent with the data shown in Fig. 8.

There is every reason to believe that the monoterpenes will experience yield enhancement in later generations. Indeed, recent findings concerning oligomerization following initial SOA formation,[7,8] as well as secondary chemical effects driven by radical chemistry following OH scavenging,[44] are examples of second-generation products influencing SOA yields. One very interesting, fundamental mechanistic aspect of the heterogeneous chemistry is the potential difference in mechanisms between gas-phase and condensed-phase oxidation subsequent to OH attack. While organo-peroxy radical cross reactions in the gas phase do not produce peroxides ($RO_2 + RO_2 \rightarrow ROOR + O_2$), if this were to occur in the condensed phase, promoted by solvent caging, it could be a significant source of cross-linking and oligomerization. However, as it is a second-order process it is likely to be extremely sensitive to both the absolute radical flux and the particle composition.

Developing a fundamental understanding of this process is a truly daunting challenge. We must consider both gas and condensed phases, through successive generations of oxidation, in a wide variety of ambient conditions (especially NO_x levels). However, fundamental understanding at critical branch points, wedded to an overall parameterization containing the essential physics and chemistry of the process, may indeed deliver a meaningful and accurate model in finite time.

8. Conclusions

There would seem to be a great separation between the questions of barrier height control raised at the beginning of this article and the questions of aerosol yields through successive generations of heterogeneous oxidation raised at the end, but these questions remain tightly coupled. From a practical perspective it is impossible to imagine obtaining detailed knowledge of every reaction depicted in Fig. 9. However, critical branch points must be studied in detail. We must understand *why* certain reactions are faster than others – why the sesquiterpene ozone reaction is anomalously fast, and why certain molecules oxidize in the condensed phase more rapidly than others. Only quantitative understanding will permit extrapolation to other systems with any confidence. We must understand why aerosol yields vary with VOC/NO_x. Again, only quantitative understanding will permit accurate extrapolation.

A key finding from current studies of heterogeneous oxidation is that experimental model systems *must* reproduce the essential complexity of real ambient aerosol, as this clearly influences oxidation kinetics. However, experiments to identify *what* part of the complex ambient matrix exerts that influence are critically needed. Overall, we see a case for the middle ground: experiments covering intermediate timescales connecting single elementary reactions with complex reaction mechanisms, and experiments covering intermediate complexity in heterogeneous systems.

Acknowledgements

This work was supported by grants from the National Science Foundation (ATM-0125283) and the US EPA (RD-83108101). Although the research described in this article has been funded wholly or in part by the United States Environmental Protection Agency through grant RD-83108101 it has not been subjected to the Agency's required peer and policy review and therefore does not necessarily reflect the views of the Agency and no official endorsement should be inferred.

References

1 R. J. Atkinson, *J. Phys. Chem. Ref. Data*, 1997, **26**, 215.
2 J. Calvert, R. Atkinson, J. Kerr, S. Madronich, G. Moortgat, T. Wallington and G. Yarwood, *The Mechanisms of Atmospheric Oxidation of the Alkenes*, Oxford University Press, New York, NY, 2000.
3 B. Chuong, J. Zhang and N. M. Donahue, *J. Am. Chem. Soc.*, 2004, **126**, 12363.

4 P. D. Carlo, W. H. Brune, M. Martinez, H. Harder, R. Lesher, X. Ren, T. Thornberry, M. A. Carroll, V. Young, P. B. Shepson, D. Riemer, E. Apel and C. Campbell, *Science*, 2004, **304**, 722.
5 M. Kulmala, K. Hameri, J. M. Makela, L. Pirjola, E. D. Nilsson, G. Buzorius, U. Rannik, M. Dal Maso, W. Seidl, T. Hoffman, R. Janson, H. C. Hansson, Y. Viisanen, A. Laaksonen and C. D. O'Dowd, *Tellus, Ser. B*, 2001, **53**, 324.
6 S. Hatakeyama, K. Izumi, T. Fukuyama and H. Akimoto, *J. Geophys. Res.*, 1989, **94**, 13013.
7 M. Klaberer, D. Paulsen, M. Sax, M. Steinbacher, J. Dommen, S. Prevot, R. Fisseha, E. Wingartner, V. Frankevich and R. U. B. Zenobi, *Science*, 2004, **303**, 1659.
8 M. Tolocka, M. Jang, J. Ginter, F. Cox, R. Kamens and M. Johnston, *Environ. Sci. Technol.*, 2004, **38**, 1428.
9 E. V. Avzianova and P. A. Ariya, *Int. J. Chem. Kin.*, 2002, **34**, 678.
10 T. Moise and Y. Rudich, *J. Geophys. Res.*, 2000, **105**, 14667.
11 J. W. Morris, P. Davidovits, J. T. Jayne, J. L. Jiminez, Q. Shi, C. E. Kolb, D. R. Worsnop, W. S. Barney and G. Cass, *Geophys. Res. Lett.*, 2002, **29**, 71.
12 G. D. Smith, I. Ephraim Woods, C. L. Deforest, T. Baer and R. E. Miller, *J. Phys. Chem. A*, 2002, **106**, 8085.
13 N. M. Donahue, J. S. Clarke and J. G. Anderson, *J. Phys. Chem. A*, 1998, **102**, 3923.
14 N. M. Donahue, *J. Phys. Chem. A*, 2001, **105**, 1489.
15 N. M. Donahue, *Chem. Rev.*, 2003, **103**, 4593.
16 S. Paulson, J. Fenske, K. Kuwata and K. N. Houk, *J. Phys. Chem. A*, 2000, **104**, 7246.
17 P. Ziemann, *J. Phys. Chem. A*, 2002, **106**, 4390.
18 R. Atkinson, S. M. Aschmann, J. Arey and J. Tuazon, *J. Phys. Chem. A*, 2003, **107**, 2247.
19 J. H. Kroll, S. Shahai, J. Anderson, K. L. Demerjian and N. Donahue, *J. Phys. Chem. A*, 2001, **105**, 4446.
20 A. A. Presto and N. M. Donahue, *J. Phys. Chem. A*, 2004, **108**, 9096.
21 A. S. Hasson, G. Orzechowska and S. E. Paulson, *J. Geophys. Res.*, 2001, **106**, 34131.
22 A. S. Hasson, A. W. Ho, K. T. Juwata and S. E. Paulson, *J. Geophys. Res.*, 2001, **106**, 34143.
23 R. J. Griffin, D. Dabdub and J. H. Seinfeld, *J. Geophys. Res.*, 2002, **107**, 4332.
24 M. Kalberer, J. Yu, D. R. Cocker, C. Flagan and J. H. Seinfeld, *Environ. Sci. Technol.*, 2000, **34**, 4894.
25 N. M. Donahue, K. Demerjian and J. Anderson, *J. Phys. Chem.*, 1996, **100**, 17855.
26 M. Sprengnether, K. L. Demerjian, N. M. Donahue and J. G. Anderson, *J. Geophys. Res. A*, 2002, **107**, ACH 8-1.
27 J. Pankow, *Atmos. Environ.*, 1994, **28**, 185.
28 J. Yu, D. R. C. R. Griffin, R. Flagan, J. Seinfeld and P. Blanchard, *J. Atm. Chem.*, 1999, **34**, 207.
29 C. O. Stanier and S. N. Pandis, *Environ. Sci. Technol.*, 2004, submitted.
30 Q. Zhang, C. Stanier, M. Caragaratna, J. T. Jayne, D. Worsnop, S. N. Pandis and J. L. Jimenez, *Environ. Sci. Technol.*, 2004, **38**, 4797.
31 B. P. S. Y. Wu, S. Seigneur, J. H. Seinfeld, R. J. Griffin and S. N. Pandis, *Environ. Sci. Technol.*, 2004, submitted.
32 S. Pandis, S. Paulson, J. Seinfeld and R. Flagan, *Atmos. Environ., Part A*, 1992, **26**, 2269.
33 A. A. Presto, K. E. Huff Hartz and N. M. Donahue, *Environ. Sci. Technol.*, 2005, submitted.
34 A. A. Presto, K. E. Huff Hartz and N. M. Donahue, *Environ. Sci. Technol.*, 2005, submitted.
35 L. M. Hilldemann, M. A. Mazurek and G. R. Cass, *Environ. Sci. Technol.*, 1991, **25**, 1311.
36 A. L. Robinson, W. Rogge and N. M. Donahue, *J. Geophys. Res.*, 2004, submitted.
37 S. A. McKeen and S. C. Liu, *Geophys. Res. Lett.*, 1993, **20**, 2363.
38 P. Ziemann, *Faraday Discuss.*, 2005, **130**, DOI: 10.1039/b417502f.
39 C. N. Cruz and S. N. Pandis, *Atmos. Environ.*, 1997, **31**, 2205.
40 T. M. Raymond and S. N. Pandis, *J. Geophys. Res.*, 2002, **107**, 4787.
41 K. E. H. Hartz, J. E. Tischuk, M. N. Chan, C. K. Chan, N. M. Donahue and S. N. Pandis, *Atmos. Environ.*, 2004, submitted.
42 K. E. H. Hartz, T. Rosenørn, S. R. Ferchak, T. M. Raymond, M. Bilde, N. M. Donahue and S. N. Pandis, *J. Geophys. Res.*, 2004, submitted.
43 M. Claeys, B. Graham, G. Vas, W. Wang, R. Vermeylen, V. Pashynska, J. Cafmeyer, P. Guyon, M. O. Andreae and P. A. W. Maenhaut, *Science*, 2004, **303**, 1173.
44 M. Keywood, J. Kroll, V. Varutbangkul, R. Bahreini, R. Flagan and J. Seinfeld, *Environ. Sci. Technol.*, 2004, **38**, 3343.